Article

Cell Reports

Histone H3 Serine 28 Is Essential for Efficient Polycomb-Mediated Gene Repression in *Drosophila*

Graphical Abstract

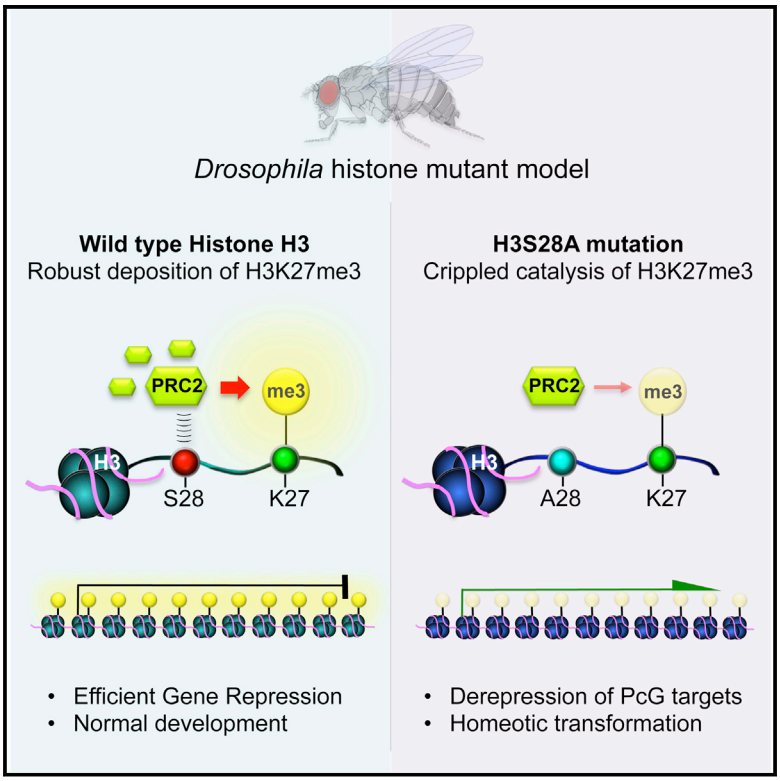

Authors

Philip Yuk Kwong Yung, Alexandra Stuetzer, ..., Anne-Marie Martinez, Giacomo Cavalli

Correspondence

wfischl@gwdg.de (W.F.), anne-marie.martinez@igh.cnrs.fr (A.-M.M.), giacomo.cavalli@igh.cnrs.fr (G.C.)

In Brief

Yung et al. establish a *Drosophila* histone mutant carrying the *H3S28A* substitution, which depletes H3S28ph without affecting mitosis. In contrast, H3K27 methylation levels decrease and polycomb silencing is strongly compromised. A combination of genetics and biochemical approaches reveal a key role of the H3S28 residue in promoting PRC2-dependent methylation at H3K27.

Highlights

- *Drosophila H3S28A* mutation supports normal mitosis despite the lack of H3S28ph
- *H3S28A* mutant shows reduced H3K27 methylation and compromises polycomb silencing
- *H3S28A* defects are not caused by active H3K27 demethylation or by loss of H3S28ph
- H3S28A reduces the ability of PRC2 to methylate H3K27 on nucleosomal substrates

Yung et al., 2015, Cell Reports *11*, 1437–1445
June 9, 2015
http://dx.doi.org/10.1016/j.celrep.2015.04.055

Cell Reports
Article

Histone H3 Serine 28 Is Essential for Efficient Polycomb-Mediated Gene Repression in *Drosophila*

Philip Yuk Kwong Yung,[1] Alexandra Stuetzer,[2] Wolfgang Fischle,[2,*] Anne-Marie Martinez,[1,3,*] and Giacomo Cavalli[1,*]
[1]Institute of Human Genetics, UPR1142 CNRS, 141 Rue de la Cardonille, 34396 Montpellier Cedex 5, France
[2]Laboratory of Chromatin Biochemistry, Max Planck Institute for Biophysical Chemistry, Am Fassberg 11, 37077 Göttingen, Germany
[3]Université de Montpellier, Place Eugène Bataillon, 34095 Montpellier Cedex 5, France
*Correspondence: wfischl@gwdg.de (W.F.), anne-marie.martinez@igh.cnrs.fr (A.-M.M.), giacomo.cavalli@igh.cnrs.fr (G.C.)
http://dx.doi.org/10.1016/j.celrep.2015.04.055

SUMMARY

Trimethylation at histone H3K27 is central to the polycomb repression system. Juxtaposed to H3K27 is a widely conserved phosphorylatable serine residue (H3S28) whose function is unclear. To assess the importance of H3S28, we generated a *Drosophila* H3 histone mutant with a serine-to-alanine mutation at position 28. *H3S28A* mutant cells lack H3S28ph on mitotic chromosomes but support normal mitosis. Strikingly, all methylation states of H3K27 drop in *H3S28A* cells, leading to Hox gene derepression and to homeotic transformations in adult tissues. These defects are not caused by active H3K27 demethylation nor by the loss of H3S28ph. Biochemical assays show that H3S28A nucleosomes are a suboptimal substrate for PRC2, suggesting that the unphosphorylated state of serine 28 is important for assisting in the function of polycomb complexes. Collectively, our data indicate that the conserved H3S28 residue in metazoans has a role in supporting PRC2 catalysis.

INTRODUCTION

Polycomb group (PcG) proteins are epigenetic regulators essential for repression of key developmental genes. Canonical targets of PcG proteins include the Hox genes, which specify the identities of body segments along the anterior to posterior axis. PcG mutants fail to maintain repressive chromatin states, leading to derepression of Hox genes and to homeotic transformations (Di Croce and Helin, 2013; Grossniklaus and Paro, 2014; Margueron and Reinberg, 2011; Schuettengruber et al., 2007; Simon and Kingston, 2013). *Drosophila* PcG proteins assemble into at least five different multiprotein complexes, namely polycomb repressive complex 1 (PRC1) (Shao et al., 1999), PRC2 (Cao et al., 2002; Czermin et al., 2002; Kuzmichev et al., 2002; Müller et al., 2002), pho-repressive complex (Pho-RC) (Klymenko et al., 2006), dRing-associated factor (dRAF) (Lagarou et al., 2008), and polycomb repressive deubiquitinase (PR-DUB) (Scheuermann et al., 2010). Enhancer of zeste, E(z), the catalytic subunit of PRC2 methylates the lysine 27 residue of histone H3 (H3K27me) on target chromatin regions. dRing is an active E3 ligase subunit in dRAF that monoubiquitinates nucleosomal H2A. In the canonical model, H3K27me3 binding by the chromodomain of polycomb helps to recruit PRC1 to target genes (Cao et al., 2002; Fischle et al., 2003; Kuzmichev et al., 2002; Min et al., 2003). Recent studies suggest an alternative recruitment hierarchy whereby H2Aub initiates PRC2 chromatin targeting and the establishment of H3K27me3 domains (Blackledge et al., 2014; Cooper et al., 2014; Kalb et al., 2014).

The local chromatin environment modulates the repressive functionality of PcG complexes (Müller and Verrijzer, 2009; O'Meara and Simon, 2012). For example, both H3K27me3 (Margueron et al., 2009) and H2Aub (Kalb et al., 2014) stimulate PRC2 activity, whereas active histone marks such as H3K4me3 and H3K36me3 (Schmitges et al., 2011) inhibit its function. Notably, the serine residue juxtaposed to H3K27, H3S28, is widely conserved and present in every species that has a canonical PRC2-dependent silencing system (Figure S1A). In contrast, it is absent in species like fission yeast that do not possess PRC2. H3S28 is mainly phosphorylated during mitosis (Giet and Glover, 2001), but whether this mitotic phosphorylation is required for mitosis in metazoans is unknown. Interphase H3S28ph has also been detected in mammals, where it was shown to counteract mammalian PRC1 and PRC2 chromatin binding. This mark derepresses PcG target genes in response to stress and developmental signaling (Gehani et al., 2010; Lau and Cheung, 2011) and activates stress response genes via displacement of HDAC corepressor complexes (Sawicka et al., 2014). However, biochemical studies showed that H3K27me3S28ph is refractory to demethylation by UTX (Sengoku and Yokoyama, 2011) and JMJD3 (Kruidenier et al., 2012). Hence, on one hand, H3S28ph might evict PcG proteins, and on the other hand, it might preserve H3K27me3. H3S28ph is established by the mitotic Aurora B kinase and, like H3S10ph, it is highly enriched during the course of mitosis (Giet and Glover, 2001). As such, H3S28ph might play a role in PcG repression and epigenetic inheritance. However, whether this is the only function of H3S28 remains unknown. In particular, the putative in vivo function of its non-phosphorylated state has not been investigated.

To assess the importance of the highly conserved H3S28 residue and to investigate the physiological relevance of mitotic H3S28ph in modulating PcG repression, we have established an in vivo *Drosophila* model where the endogenous source of

histone H3 is replaced by a non-phosphorylatable serine 28 to alanine mutation. Surprisingly, this mutation did not significantly affect mitosis. However, methylation of H3K27 was severely impaired and polycomb-mediated silencing of Hox genes was partially lost, resulting in homeotic transformations in the adults. The deregulation of PcG silencing associated with *H3S28A* mutation is independent of active demethylation and cannot be recapitulated upon the loss of Aurora B kinase. These observations are consistent with in vitro experiments showing that PRC2 activity is impaired upon H3 serine to alanine mutation at position 28 (*H3S28A*). Collectively, our data suggest that one main function of H3S28 is to support polycomb-mediated silencing via PRC2-dependent methylation of H3K27.

RESULTS

All H3K27 Methylation States Are Reduced in the *H3S28A* Mutant

In the *Drosophila* genome, canonical core and linker histones are encoded by the histone gene unit (HisGU), which is organized as a multicopy gene array residing at a single locus known as the histone gene cluster (*HisC*). Previous studies showed that embryos carrying homozygous *HisC* deletion (*ΔHisC*) die in late blastoderm, after exhaustion of maternally deposited histone reserves (Günesdogan et al., 2010; McKay et al., 2015). A histone replacement genetic platform has been developed based on the fact that reintroduction of a minimum of 12 copies of wild-type transgenic HisGU is sufficient to rescue lethality of the *ΔHisC* mutant. Likewise, HisGU carrying different point mutations can be introduced in this system to study the biological functions of specific histone residues and modifications thereof (Günesdogan et al., 2010). In a previous study, an *H3K27R* mutant was analyzed (McKay et al., 2015; Pengelly et al., 2013). It was reported that the limited number of cell divisions during late embryogenesis was not sufficient to completely replace wild-type, chromatinized maternal histones, resulting in chromatin with a mixture of wild-type and mutant histones. To circumvent this limitation, mosaic analysis of histone mutants was developed with the use of FLP-FRT-mediated recombination (Figure S1B). This way, homozygous *ΔHisC* clones are detected when they are supplemented with 12×HisGU of either WT or mutated histones in larval tissues (Hödl and Basler, 2012; Pengelly et al., 2013). We adopted the same system to generate a *H3S28A* mutant. In parallel, histone replacement lines carrying *WT* and *H3K27R* histone mutants were established as controls. This system replaces all canonical histones, leaving the endogenous genes coding for the histone variant H3.3 (*His3.3A* and *His3.3B*) intact. To simplify the nomenclature, we refer to homozygous *ΔHisC* clones supplemented with different transgenic 12×HisGU as *WT*, *H3S28A*, and *H3K27R* lines, unless otherwise stated.

Consistent with previous reports (Hödl and Basler, 2012; Pengelly et al., 2013), homozygous *ΔHisC* clones (lacking GFP) induced with a heat shock pulse of FLP died (data not shown). Reintroducing 12×HisGU in the form of WT-H3, H3S28A, or H3K27R mutants displayed DAPI and H3 staining patterns similar to the neighboring GFP-positive tissues (Figures 1 and S1C). Importantly, *H3S28A* clones specifically lost the mitotic H3S28ph signal, whereas they retained normal levels of H3S10ph (Figure 1B). Likewise and as previously reported (McKay et al., 2015; Pengelly et al., 2013), *H3K27R* clones almost completely lost the H3K27me3 mark, without affecting neighboring mitotic phosphorylation at H3S28 (Figure S1D). These results imply that the native pool of histone variant H3.3 neither supports mitotic H3S28ph nor H3K27me3. This may be linked to the transcription-coupled deposition pathway of H3.3, which restricts its distribution to active promoters, resulting in genomic distributions that might not be compatible with PRC2 catalysis. Importantly, mitotic H3S10ph, H3S28ph, and H3K27me3 signals were not affected in *WT* clones (Figures 1A, 1C, and S1D).

Because H3K27 and H3S28 are adjacent to each other, and as H3S28ph was shown to evict PcG components (Gehani et al., 2010; Lau and Cheung, 2011) and to prevent H3K27me demethylation (Kruidenier et al., 2012; Sengoku and Yokoyama, 2011), we asked whether the loss of H3S28ph in *H3S28A* clones affects H3K27 methylation. Strikingly, H3K27me3 and H3K27me1 were strongly reduced in *H3S28A* clones (Figure 1D). Considerable reduction of H3K27me2 was also detected. This was in stark contrast to active chromatin marks, where H3K27ac was only mildly decreased and H3K4me3 was unaffected in *H3S28A* clones. As a control, *WT* clones showed normal staining levels indistinguishable from neighboring tissues for all histone marks examined (Figure 1C). These findings show that H3S28 is specifically required for PRC2 function in vivo.

H3S28A and *H3K27R* Mutants Both Cause Derepression of Hox Genes

In various PRC2 mutants (Beuchle et al., 2001; Birve et al., 2001; Müller et al., 2002), as well as in the *H3K27R* histone mutant clones where H3K27me3 levels are compromised (McKay et al., 2015; Pengelly et al., 2013), canonical PcG targets such as Hox genes are derepressed. Hence, we analyzed Hox gene expression in the *H3S28A* mutant in comparison to the *H3K27R* mutant.

Endogenous expression of Scr is limited to a patch of cells located at the base of antennal discs (asterisks) and is absent within the antennal disc proper (Abzhanov et al., 2001). Scr was derepressed across the entire antennal disc in both *H3S28A* and *H3K27R* mutant clones (Figure 2A). In line with a previous report (Pattatucci and Kaufman, 1991), low levels of endogenous Scr expression were observed in the adepithelial cells of the second and third leg discs (Figure S2A, asterisks). We observed strong derepression of Scr in *H3S28A* and *H3K27R* mutant clones of these tissues (Figure S2A). Moreover, Scr derepression was occasionally detected in the notum region of wing discs in both histone mutant clones (Figure S2A), similar to what was previously reported in Pc^3/+ heterozygous mutant background (Pattatucci and Kaufman, 1991).

We also detected strong derepression of Ubx in antennal and wing discs of both *H3S28A* and *H3K27R* mutant clones (Figures 2A and S2A). Ubx derepression was mainly restricted to the wing pouch region at a level comparable to its native expression in the haltere disc. For Abd-B, strong derepression was detected in *H3K27R* clones across the entire eye-antennal and wing discs (Pengelly et al., 2013), whereas *H3S28A* clones showed no obvious derepression in the same tissues (Figures 2A and S2A), suggesting that the partial loss of H3K27me3 was not

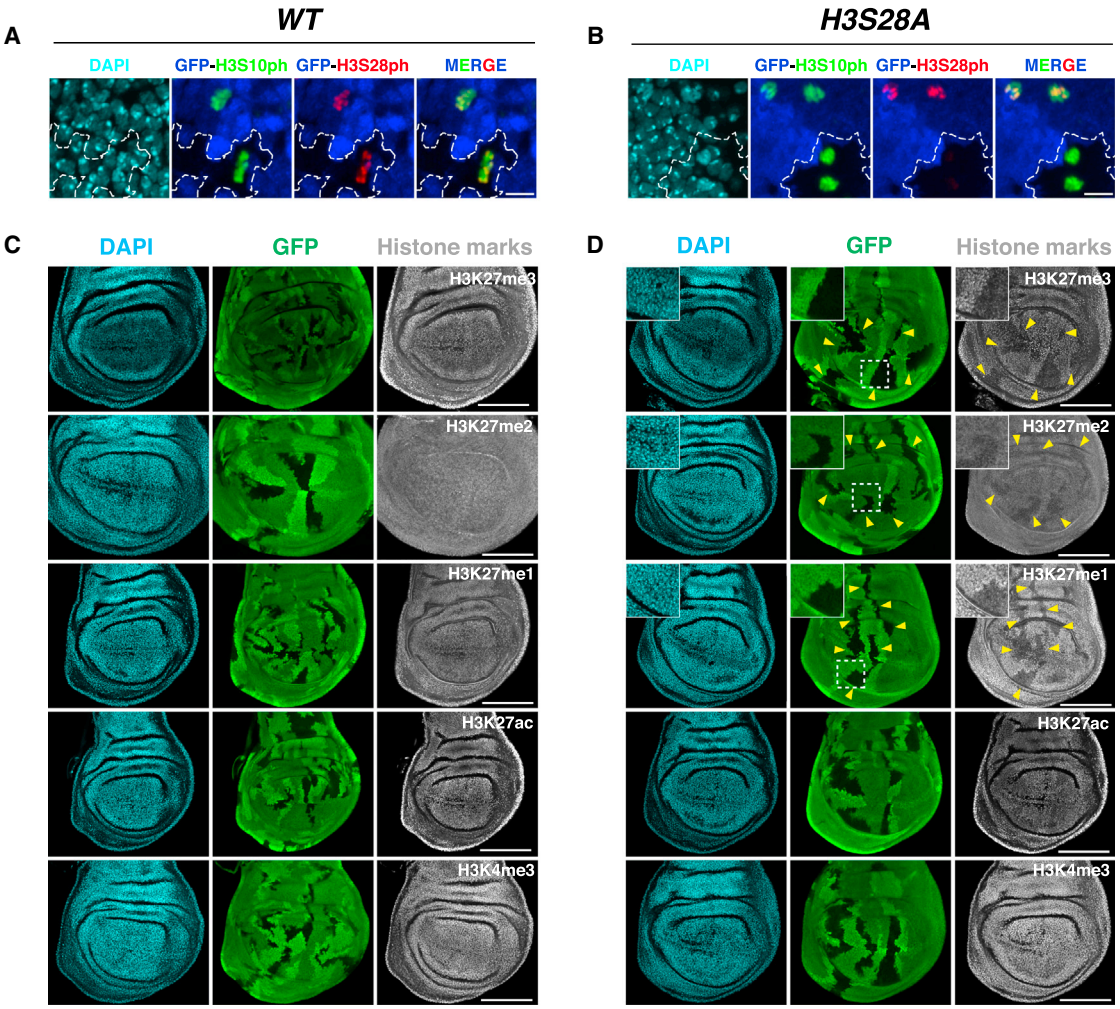

Figure 1. *H3S28A* Mutant Specifically Depletes Mitotic H3S28ph and Compromises All H3K27 Methylation States

Eye-antenna (A and B) or wing (C and D) imaginal discs of the indicated histone replacement genotype. Immunostaining with the indicated antibodies is shown; DNA was stained with DAPI. Clones of interest were marked by the lack of GFP signal and are indicated by dashed lines. (A and B) H3S10ph (green) and H3S28ph (red) levels are shown in mitotic cells from GFP-negative (histone replacement) clones as well as GFP-positive normal tissue. (C) and (D) Arrowheads highlight *H3S28A* clones with considerable drop in H3K27 methylation levels. Insets represent the magnified region indicated by dashed lines. For clarity of composite micrographs, GFP is pseudocolored to blue in (A) and (B). In order to capture mitotic cells at different focal planes, a Z projection is applied in (A) and (B). The scale bars in (A) and (B) correspond to 5 μm, whereas those in (C) and (D) correspond to 100 μm. See also Figure S1.

sufficient to induce Abd-B derepression in *H3S28A* clones. No changes in expression of Hox genes were detected in the imaginal discs of WT-H3 clones.

In addition to the aforementioned Hox genes, we observed derepression of Antp in the antennal discs of *H3S28A* and *H3K27R* mutant clones (Figures 2B and S2A). Similar to the $Antp^{Ns}$ mutant with ectopic expression of Antp in the antennal disc (Figure S2B), GAL4-driven overexpression of various Hox genes in the antennal disc is known to silence the antennal selector gene Hth and cause antenna-to-leg transformation (Yao et al., 1999). In agreement with this observation, the *H3S28A* and *H3K27R* clones also showed Hth silencing, which was most prominent in the *H3K27R* mutant (Figure 2B).

Because Hox gene derepression can induce homeotic transformations, we investigated the phenotypic consequence of the induction of *H3S28A* or *H3K27R* clones in adults. Consistent with the Hox derepression and Hth silencing phenotypes in larval tissues, adult flies developing from clonal *H3S28A* and *H3K27R* mutant backgrounds displayed antenna-to-leg transformation. Wild-type *Drosophila* adults showed distinct antenna segmentation into a1–a3 and arista, as annotated on w^{1118} in Figure 2C. Notably, the *H3K27R* mutant displayed an enlarged a3 antennal segment, from which massive outgrowth developed with leg-like features. This resembled the *antennapedia* phenotype of the $Antp^{Ns}$ mutant. The *H3S28A* mutant showed milder transformations, with smaller a3 segment protrusions and thickening of arista resembling the *aristapedia* phenotype. In contrast, WT histone replacement flies showed normal antenna structures (Figure 2C).

In summary, the partial loss of H3K27me3 in the *H3S28A* mutant induces loss of polycomb silencing, although the effects

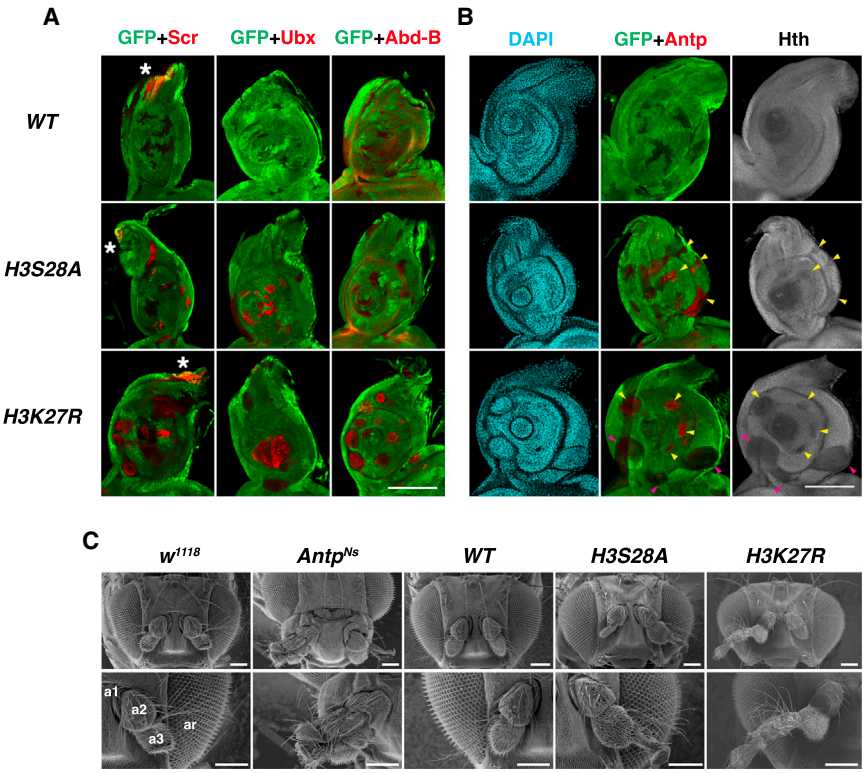

Figure 2. Deregulation of Hox and Antenna Selector Genes in *H3S28A* and *H3K27R* Mutants and Their Associated Transformation Phenotypes

(A and B) Antennal discs with *WT*, *H3S28A*, and *H3K27R* clones were immunostained with anti-GFP and the indicated antibodies. DNA was stained with DAPI. Mutant clones are marked by the absence of GFP signal. The scale bars in antennal discs represent 100 μm. (A) The expression of Scr (left), Ubx (center), and Abd-B (right) in the antennal discs is shown in the indicated histone mutant background. Endogenous expression of Scr is marked by asterisks. (B) The expression of Antp and Hth in the antennal discs is shown in the indicated histone mutant background. Clones with derepressed Antp and silenced endogenous Hth expressions are marked by yellow arrowheads; those with silenced Hth but without Antp derepression are marked by magenta arrowheads.

(C) Electron micrographs of adult *Drosophila* heads derived from w^{1118}, $Antp^{Ns}$, and the indicated mosaic histone replacement lines. Normal segmented antenna structures are annotated as a1, a2, a3, and ar (arista). $Antp^{Ns}$ was shown as a positive control for antenna-to-leg transformation. The scale bars correspond to 100 μm.

See also Figures S2 and S4.

were milder than those of the *H3K27R* mutant, as indicated by Abd-B staining, which only shows derepression in *H3K27R* clones (Figures 2A and S2A).

Deregulation of PcG Silencing in *H3S28A* Mutant Is Independent of Active Demethylation and Cannot Be Recapitulated by Depletion of Aurora B Kinase

We investigated the mechanistic basis for the loss of silencing induced by the *H3S28A* mutation. Because H3S28ph was shown to evict PcG protein binding to H3K27me3 but also to prevent H3K27me3 demethylation, one explanation for the observed deregulation in PcG silencing in *H3S28A* mutant could be active H3K27me demethylation upon the loss of H3S28ph. If this was correct, combining *dUtx*-null background with the *H3S28A* mutation should alleviate the reduction of H3K27me levels and PcG-silencing defects. By recombining *dUtxΔ* mutation (Copur and Müller, 2013) with *ΔHisC*, we generated double homozygous mutants by recombination over a single FRT element. As shown in Figure S3A, the *dUtxΔ*, *H3S28A* mutant clone is depleted of dUtx. However, all H3K27 methylation states are not rescued under such condition (Figure 3A). We also tested the possibility that the *H3S28A* phenotype is a consequence of the absence of H3S28 phosphorylation. We therefore induced RNAi against the Aurora B kinase in the wing imaginal disc. This resulted in robust depletion of Aurora B (Figure S3B) and mitotic H3S10ph and H3S28ph (Figure S3C). Consistent with previous reports, loss of Aurora B caused aneuploidy and enlarged nuclei (Giet and Glover, 2001). If the decrease in H3K27me and the loss of Hox gene silencing observed in the *H3S28A* mutant was depending on the absence of H3S28 phosphorylation, one would expect to observe these phenotypes upon loss of Aurora B. In contrast, we did not observe reduction of H3K27me3 levels or *Ubx* derepression in the knockdown region of wing discs (Figure 3B). Taken together, these data suggest that demethylation by dUtx and the loss of H3S28 phosphorylation per se do not compromise polycomb silencing in the *H3S28A* mutant.

H3S28A Impairs H3K27 Methylation of Nucleosomes by PRC2

Together, the results described above suggested the possibility that the serine-to-alanine substitution per se might affect PRC2 activity. To directly test this hypothesis, we performed in vitro histone methyltransferase (HMT) assays using a reconstituted, four-component core *Drosophila* PRC2 complex that includes Esc, Su(z)12, E(z), and Nurf55 (Müller et al., 2002; Schmitges et al., 2011). As shown by previous reports (Margueron et al., 2009; Schmitges et al., 2011), when assayed on WT nucleosomes supplied with a *trans*-acting histone peptide carrying H3K27me3, PRC2 activity was robustly enhanced in a dose-dependent manner (Figure 4). Only basal HMT activities were detected when H3S28ph, unmodified, or no histone peptides were added to the reaction mixtures. Interestingly, the stimulatory effect of H3K27me3 was retained when combined with the H3S28A mutation (H3K27me3S28A; Figure 4A). By contrast, the PRC2-stimulatory activity was abolished in context of the H3K27me3S28ph "double mark" (Figure 4A). Available structural data show that the stimulatory effect relies on the binding

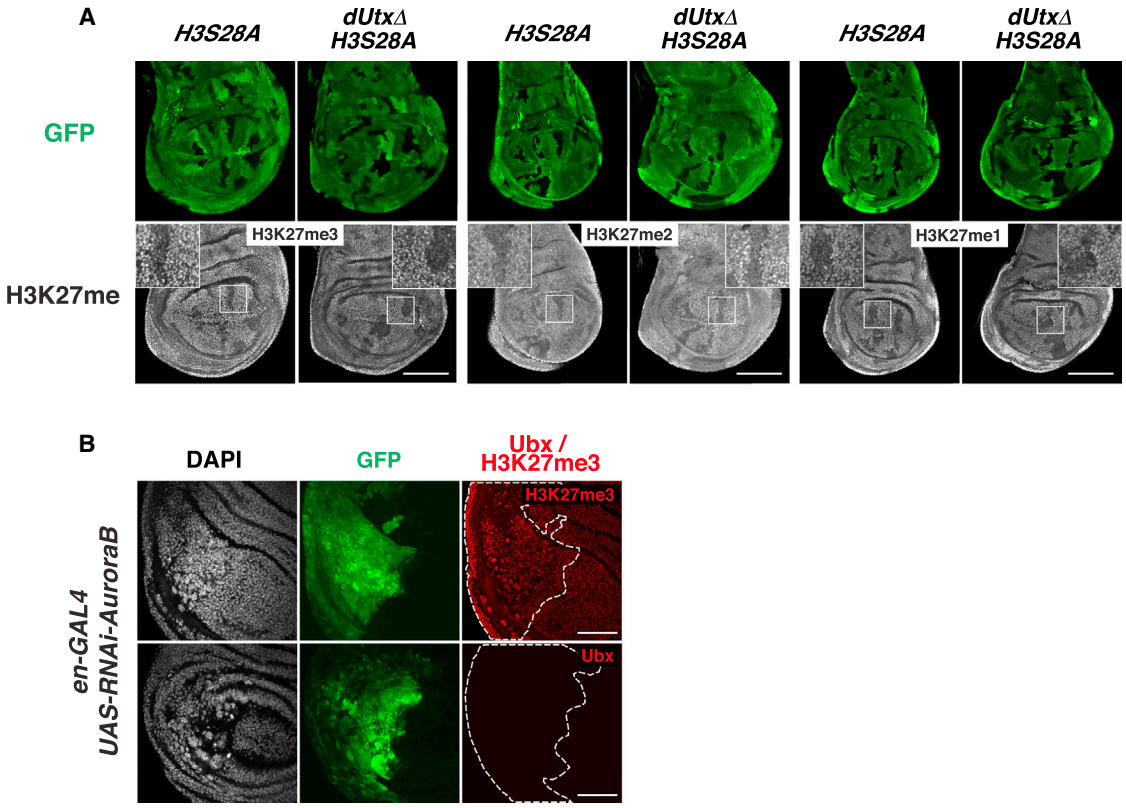

Figure 3. *dUtxΔ*, *H3S28A* Double Mutant Does Not Rescue H3K27 Methylation Levels, and Loss of Aurora B Kinase Does Not Perturb Polycomb Silencing

(A) Wing discs carrying clones with either *H3S28A* alone or in combination with *dUtxΔ* were immunostained with the indicated antibodies.

(B) Wing discs of L3 larvae with *en-GAL4* directed RNAi against Aurora B at the posterior compartment (knocked down cells are in the region marked by GFP and dotted lines) were immunostained with the indicated antibodies. DNA was stained with DAPI. The scale bars correspond to 100 μm.

See also Figure S3.

of H3K27me3 to the beta-propeller structure of Esc with the side chain of H3S28 pointing away from the binding side (Margueron et al., 2009; O'Meara and Simon, 2012). Apparently, this interaction is not affected by the loss of the hydroxyl group in the serine-to-alanine substitution in H3K27me3S28A peptides. However, the introduction of the more-bulky and charged phosphate group on H3S28 prevents any stimulatory effect. We assume that this is due to hampered binding of the H3K27me3S28ph peptide to Esc.

We then performed PRC2 HMT assays with H3S28A mutant nucleosomes. In this context, enzymatic activity was considerably reduced, with or without supplementation of stimulatory H3K27me3-containing peptides in trans (Figure 4B). Similar to WT nucleosomal substrates, the stimulatory effect of H3K27me3 and H3K27me3S28A peptides was comparable on H3S28A nucleosomes. Therefore, the H3S28A effect can be ascribed to inhibition of PRC2-dependent methylation of H3K27.

DISCUSSION

In this report, we have established a *H3S28A* histone mutant in *Drosophila*. In theory, this mutation could have two different effects on the polycomb system. (1) It could be that PcG proteins are not evicted from H3K27me3-binding sites in the absence of H3S28ph, and thus, PcG target genes might become ectopically repressed or (2) the mutation at H3S28 or the absence of H3S28ph could compromise PcG functions, resulting in derepression of PcG target genes. We found no evidence for the first possibility, although it is formally possible that H3S28 is phosphorylated under certain developmental conditions or in response to particular stimuli to counteract polycomb silencing. Instead, our data point to an inhibition of PRC2 activity by the *H3S28A* mutation. This inhibition is independent of active H3K27 demethylation by dUtx. Besides, RNAi against Aurora B kinase and hence depletion of H3S28ph did not hamper polycomb silencing. On the other hand, H3S28A nucleosomes proved to be a suboptimal substrate for in vitro PRC2 HMT activity. Although a 3D structure of the human Ezh2 SET domain is available (Antonysamy et al., 2013), the exact contribution of the hydroxyl group of H3S28 for H3K27 methylation is difficult to deduce from the available data. vSET, the only other protein capable of H3K27 methylation in the absence of PRC2 subunits, does not require H3S28 for catalysis, whereas it does use H3A29 to define substrate specificity (Wei and Zhou, 2010). Clearly,

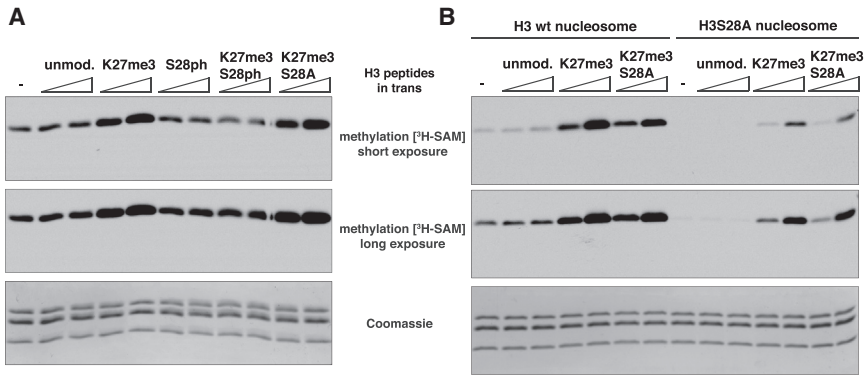

Figure 4. H3S28A Impairs H3K27 Methylation of Nucleosomes by PRC2

(A) In vitro HMT assay using reconstituted *Drosophila* PRC2 complex, WT nucleosomes, and ^{3}H-SAM as substrates. Reactions were supplied in trans with the indicated histone peptides at concentrations of 5 and 40 μM.

(B) In vitro PRC2 HMT assay as in (A) but using nucleosomal substrates assembled with either WT-H3 or H3S28A mutant protein. Reactions were separated by SDS-PAGE and analyzed by fluorography. Fluorographs with different exposures are shown. Coomassie staining of the histones serves as loading control.

more work will be required to determine the exact structural and biochemical role of H3S28 in PRC2 catalysis. Consistent with the in vitro HMT assays, in vivo the *H3S28A* mutant exhibits defects in H3K27 methylation and shows similar, though milder, Hox derepression profiles and transformation phenotypes to those observed in *H3K27R* mutant flies.

Interestingly, the "KS" module is frequently found in Ezh2 substrates other than K27S28 of histone H3. These include K26S27 of human histone H1 variant H1b (H1.4), K38S39 of the nuclear orphan receptor RORα, and K180S181 of STAT3 (Kim et al., 2013; Kuzmichev et al., 2004; Lee et al., 2012; Pasini et al., 2004). Whether these serine residues act similarly to H3S28 to support methylation of the adjacent lysine residue remains unknown. Of note, some other Ezh2 substrates can be methylated despite the lack of a "KS" module. These include K26 of mouse histone H1 variant H1e, K49 of STAT3, and K116 of Jarid2 (Dasgupta et al., 2015; Kuzmichev et al., 2004; Sanulli et al., 2015), where the lysine residue is followed by an alanine, glutamate, and phenylalanine, respectively. Moreover, the link between peptide sequence and enzymology of Ezh2 was shown to differ in non-histone substrates (Lee et al., 2012). Hence, the role of serine following the Ezh2 methylation target amino acid might not be extrapolated to all other Ezh2 substrates and should be tested individually.

Previous reports revealed discrepancies in *Drosophila* PcG protein localization on mitotic chromosomes depending on staining protocols and tissue types (Buchenau et al., 1998; Fanti et al., 2008; Follmer et al., 2012; Fonseca et al., 2012). Nonetheless, live imaging of Pc-GFP, Ph-GFP, and E(z)-GFP in early *Drosophila* embryos (Cheutin and Cavalli, 2012; Steffen et al., 2013) all suggested that the majority of these PcG components are dissociated from mitotic chromosomes. Because stress-induced H3S28ph evicts PcG complexes during interphase (Lau and Cheung, 2011; Schmitges et al., 2011), one might expect rebinding of PcG proteins on mitotic chromosomes depleted of H3S28ph. Whereas we did observe loss of Ph from mitotic chromosomes in WT background, we did not observe significant Ph association in *H3S28A* mutant condition (Figure S4). The reduced levels of H3K27me3 in the *H3S28A* mutant could contribute to this observation. Alternatively, other mechanisms might operate to dissociate the majority of PcG proteins during mitosis.

The establishment of the histone replacement system in *Drosophila* has proven to be an important tool to complement functional characterization of chromatin modifiers (Hödl and Basler, 2012; McKay et al., 2015; Pengelly et al., 2013). Whereas depletion of H3K27 methylation, either by mutation of the histone mark writer *E(z)* or by mutation of the histone itself in the *H3K27R* mutant, leads to similar loss of polycomb-dependent silencing (McKay et al., 2015; Pengelly et al., 2013), other histone mutations revealed different phenotypes than the loss of their corresponding histone mark writers. For example, *H3K4R* mutations in both H3.2 and H3.3, hence a complete loss of H3K4 methylation, did not hamper active transcription (Hödl and Basler, 2012). Also, the loss of H4K20 methylation upon *H4K20R* mutation unexpectedly supports development and does not phenocopy cell cycle and gene silencing defects reported upon the loss of the H4K20 methylase PR-Set7 (McKay et al., 2015). Here, by comparing the phenotype of Aurora B knockdown and *H3S28A* mutation in vivo, together with in vitro HMT assay, we specifically attribute the requirement of the unmodified H3S28 residue in supporting PRC2 deposition of H3K27 methylation.

Whereas the published data suggest that H3S28 phosphorylation might be important for eviction of PcG components for derepression of PcG target genes upon stimulatory cues (Gehani et al., 2010; Lau and Cheung, 2011; Sawicka et al., 2014), our data reveal a so far unacknowledged function of the unphosphorylated state of H3S28. We show that serine 28 is required to enable proper methylation of H3K27 by PRC2 and thus to establish polycomb-dependent gene silencing. Serine 28 of histone H3 is universally conserved in species that display canonical PRC2-dependent silencing mechanisms. Given the fact that we find no major mitotic defects upon its mutation, we propose that the major role of this residue is to ensure optimal PRC2 function while facilitating the removal of polycomb proteins in response to signals that induce phosphorylation.

Supplemental Information for this article is available online.

EXPERIMENTAL PROCEDURES

Plasmids

Construction of integration plasmids p*ϕC31attB3xHisGU* carrying either wild-type H3, H3K27R, or H3S28A mutation followed published procedures (Günesdogan et al., 2010). Entry vectors pENTR221-*HisGU*, pENTRL4R1-*HisGU*, pENTRR2L3-*HisGU*, and their H3K27R mutant derivatives, together with the destination vector pDESTR3R4-*ϕC31attB*, were obtained from Alf Herzig (Max-Planck-Institut für Infektionsbiologie). Gene synthesis (Eurofins

Scientific SE) of a DNA fragment carrying the codon exchange AGT→GCC introduced the H3S28A mutation. Subcloning of the H3S28A DNA fragment into entry vectors and subsequent recombineering followed the procedures published for generating the *H3K27R* mutant (Günesdogan et al., 2010).

Drosophila Stocks

Site-specific transgenesis and fly genetics were performed as previously described (Günesdogan et al., 2010). The histone deficiency mutant (*ΔHisC*) used in this study (*Df(2L)BSC104*) was obtained from Konrad Basler (Institute of Molecular Life Sciences) in the form of *Df(2L) BSC104*, *FRT40A* recombinant (Hödl and Basler, 2012). The *dUtxΔ* line was obtained from Jürg Müller (The Max Planck Institute of Biochemistry) in the form of *dUtxΔ*, *FRT40A* (Copur and Müller, 2013) recombinant.

Mosaic Analysis and Immunostaining

Egg depositions were allowed over a 24-hr time window at 25°C. Larvae developed for 2 days before they were heat shocked at 37°C for 1 hr. L3 larva emerged 3 days after heat shock, and they were selected for the lack of green balancer before dissection. Inverted larvae heads were fixed in 4% formaldehyde/PBS for 20 min at room temperature. After washing with PBS, the samples were permeabilized twice with 0.3% Triton X-100 in PBS for 30 min at room temperature. After blocking with 3% BSA 0.03% Triton X-100 in PBS for 1 hr, the samples were incubated with primary antibodies in 0.03% Triton X-100 in PBS overnight at 4°C. Samples were then incubated secondary antibodies conjugated to Alexa (Invitrogen) fluorophores before DAPI staining. Thorough washes were applied in between incubations. Imaginal discs were carefully removed and mounted with ProLong Gold (Invitrogen) antifade reagent. Micrographs were acquired on a Zeiss LSM 780 inverted confocal microscope. Raw micrographs were processed with ImageJ and assembled using Adobe Illustrator.

Scanning Electron Microscopy

Adult fly heads were fixed as described (Wolff, 2011) using the critical-point-dried method. They were then sputter-coated with a 10-nm-thick gold film and examined under a scanning electron microscope (Hitachi S4000) using a lens detector with an acceleration voltage of 10 kV at calibrated magnifications.

In Vitro PRC2 HMT Assay

Nucleosomes and chromatin arrays were reconstituted by the salt gradient dialysis method as described (Luger et al., 1999) using recombinant *Xenopus laevis* core histones. Nucleosomes contained a 187-bp-long DNA fragment with the 601 DNA sequence at its center (Munari et al., 2012). The histone mutant H3S28A was generated by site-directed mutagenesis. All reconstitutions were analyzed by native gel electrophoresis.

H3 peptides corresponding to H3 amino acids 21–33 were synthesized according to standard procedures. A non-natural tyrosine was added at the C terminus for quantification.

HMT reactions were performed using 1-μg nucleosomes in a total volume of 15 μl for 1 hr at 30°C. HMT reactions were carried out in presence of 0.8 μCi S-[methyl-^{3}H]-Adenosyl-L-methionine (^{3}H-SAM) and 325 ng PRC2 (75 nM) in HMT buffer (50 mM Tris-HCl [pH 8.8], 5 mM $MgCl_2$, and 4 mM DTT). Recombinant *Drosophila melanogaster* PRC2 complex, comprised of Su(z)12, E(z), Nurf55, and Esc, was a kind gift of Nicolas Thomä (Friedrich Miescher Institute) and was purified as described (Schmitges et al., 2011). PRC2 HMT assays in presence of $H3_{21–33}$ peptides in trans contained 5 or 40 μM of peptide. Reactions were stopped by addition of SDS sample buffer followed by separation by SDS-PAGE. Reactions were analyzed by fluorography.

More details on the experimental procedures can be found in the Supplemental Information.

SUPPLEMENTAL INFORMATION

Supplemental Information includes Supplemental Experimental Procedures and four figures and can be found with this article online at http://dx.doi.org/10.1016/j.celrep.2015.04.055.

AUTHOR CONTRIBUTIONS

P.Y.K.Y., A.-M.M., and G.C. conceived and designed the *Drosophila* experiments. A.S. performed the in vitro PRC2 HMT assays with input from W.F. P.Y.K.Y. performed all other experiments. All authors analyzed the data. P.Y.K.Y. and G.C. wrote the manuscript with help from A.S. and W.F.

ACKNOWLEDGMENTS

We are grateful to Natalia Azpiazu, Konrad Basler, Walter Gehring, David Glover, Peter J. Harte, Alf Herzig, Martina Hödl, Ginés Morata, Jürg Müller, Nicolas Thomä, and Feng Tie for providing research reagents. Boyan Bonev, Thierry Cheutin, Satish Sati, and Bernd Schuettengruber provided helpful comments on the manuscript. We thank Chantal Cazevieille for assistance with scanning electron microscopy and in the use of the Montpellier RIO imaging facility. Research in the laboratory of G.C. was supported by grants from the European Research Council (ERC-2008-AdG no. 232947), the CNRS, the European Network of Excellence EpiGeneSys, the Agence Nationale de la Recherche, and the Fondation ARC pour la Recherche sur le Cancer. Funding of P.Y.K.Y. was supported by the Croucher Foundation and La Ligue contre le Cancer. Research in the laboratory of W.F. was supported by the Max Planck Society.

Received: March 1, 2015
Revised: March 31, 2015
Accepted: April 25, 2015
Published: May 21, 2015

REFERENCES

Abzhanov, A., Holtzman, S., and Kaufman, T.C. (2001). The Drosophila proboscis is specified by two Hox genes, proboscipedia and Sex combs reduced, via repression of leg and antennal appendage genes. Development *128*, 2803–2814.

Antonysamy, S., Condon, B., Druzina, Z., Bonanno, J.B., Gheyi, T., Zhang, F., MacEwan, I., Zhang, A., Ashok, S., Rodgers, L., et al. (2013). Structural context of disease-associated mutations and putative mechanism of autoinhibition revealed by X-ray crystallographic analysis of the EZH2-SET domain. PLoS ONE *8*, e84147.

Beuchle, D., Struhl, G., and Müller, J. (2001). Polycomb group proteins and heritable silencing of Drosophila Hox genes. Development *128*, 993–1004.

Birve, A., Sengupta, A.K., Beuchle, D., Larsson, J., Kennison, J.A., Rasmuson-Lestander, A., and Müller, J. (2001). Su(z)12, a novel Drosophila Polycomb group gene that is conserved in vertebrates and plants. Development *128*, 3371–3379.

Blackledge, N.P., Farcas, A.M., Kondo, T., King, H.W., McGouran, J.F., Hanssen, L.L., Ito, S., Cooper, S., Kondo, K., Koseki, Y., et al. (2014). Variant PRC1 complex-dependent H2A ubiquitylation drives PRC2 recruitment and polycomb domain formation. Cell *157*, 1445–1459.

Buchenau, P., Hodgson, J., Strutt, H., and Arndt-Jovin, D.J. (1998). The distribution of polycomb-group proteins during cell division and development in Drosophila embryos: impact on models for silencing. J. Cell Biol. *141*, 469–481.

Cao, R., Wang, L., Wang, H., Xia, L., Erdjument-Bromage, H., Tempst, P., Jones, R.S., and Zhang, Y. (2002). Role of histone H3 lysine 27 methylation in Polycomb-group silencing. Science *298*, 1039–1043.

Cheutin, T., and Cavalli, G. (2012). Progressive polycomb assembly on H3K27me3 compartments generates polycomb bodies with developmentally regulated motion. PLoS Genet. *8*, e1002465.

Cooper, S., Dienstbier, M., Hassan, R., Schermelleh, L., Sharif, J., Blackledge, N.P., De Marco, V., Elderkin, S., Koseki, H., Klose, R., et al. (2014). Targeting polycomb to pericentric heterochromatin in embryonic stem cells reveals a role for H2AK119u1 in PRC2 recruitment. Cell Rep. *7*, 1456–1470.

Copur, Ö., and Müller, J. (2013). The histone H3-K27 demethylase Utx regulates HOX gene expression in Drosophila in a temporally restricted manner. Development *140*, 3478–3485.

Czermin, B., Melfi, R., McCabe, D., Seitz, V., Imhof, A., and Pirrotta, V. (2002). Drosophila enhancer of Zeste/ESC complexes have a histone H3 methyltransferase activity that marks chromosomal Polycomb sites. Cell *111*, 185–196.

Dasgupta, M., Dermawan, J.K., Willard, B., and Stark, G.R. (2015). STAT3-driven transcription depends upon the dimethylation of K49 by EZH2. Proc. Natl. Acad. Sci. USA *112*, 3985–3990.

Di Croce, L., and Helin, K. (2013). Transcriptional regulation by Polycomb group proteins. Nat. Struct. Mol. Biol. *20*, 1147–1155.

Fanti, L., Perrini, B., Piacentini, L., Berloco, M., Marchetti, E., Palumbo, G., and Pimpinelli, S. (2008). The trithorax group and Pc group proteins are differentially involved in heterochromatin formation in Drosophila. Chromosoma *117*, 25–39.

Fischle, W., Wang, Y., Jacobs, S.A., Kim, Y., Allis, C.D., and Khorasanizadeh, S. (2003). Molecular basis for the discrimination of repressive methyl-lysine marks in histone H3 by Polycomb and HP1 chromodomains. Genes Dev. *17*, 1870–1881.

Follmer, N.E., Wani, A.H., and Francis, N.J. (2012). A polycomb group protein is retained at specific sites on chromatin in mitosis. PLoS Genet. *8*, e1003135.

Fonseca, J.P., Steffen, P.A., Müller, S., Lu, J., Sawicka, A., Seiser, C., and Ringrose, L. (2012). In vivo Polycomb kinetics and mitotic chromatin binding distinguish stem cells from differentiated cells. Genes Dev. *26*, 857–871.

Gehani, S.S., Agrawal-Singh, S., Dietrich, N., Christophersen, N.S., Helin, K., and Hansen, K. (2010). Polycomb group protein displacement and gene activation through MSK-dependent H3K27me3S28 phosphorylation. Mol. Cell *39*, 886–900.

Giet, R., and Glover, D.M. (2001). Drosophila aurora B kinase is required for histone H3 phosphorylation and condensin recruitment during chromosome condensation and to organize the central spindle during cytokinesis. J. Cell Biol. *152*, 669–682.

Grossniklaus, U., and Paro, R. (2014). Transcriptional silencing by polycomb-group proteins. Cold Spring Harb. Perspect. Biol. *6*, a019331.

Günesdogan, U., Jäckle, H., and Herzig, A. (2010). A genetic system to assess in vivo the functions of histones and histone modifications in higher eukaryotes. EMBO Rep. *11*, 772–776.

Hödl, M., and Basler, K. (2012). Transcription in the absence of histone H3.2 and H3K4 methylation. Curr. Biol. *22*, 2253–2257.

Kalb, R., Latwiel, S., Baymaz, H.I., Jansen, P.W., Müller, C.W., Vermeulen, M., and Müller, J. (2014). Histone H2A monoubiquitination promotes histone H3 methylation in Polycomb repression. Nat. Struct. Mol. Biol. *21*, 569–571.

Kim, E., Kim, M., Woo, D.H., Shin, Y., Shin, J., Chang, N., Oh, Y.T., Kim, H., Rheey, J., Nakano, I., et al. (2013). Phosphorylation of EZH2 activates STAT3 signaling via STAT3 methylation and promotes tumorigenicity of glioblastoma stem-like cells. Cancer Cell *23*, 839–852.

Klymenko, T., Papp, B., Fischle, W., Köcher, T., Schelder, M., Fritsch, C., Wild, B., Wilm, M., and Müller, J. (2006). A Polycomb group protein complex with sequence-specific DNA-binding and selective methyl-lysine-binding activities. Genes Dev. *20*, 1110–1122.

Kruidenier, L., Chung, C.W., Cheng, Z., Liddle, J., Che, K., Joberty, G., Bantscheff, M., Bountra, C., Bridges, A., Diallo, H., et al. (2012). A selective jumonji H3K27 demethylase inhibitor modulates the proinflammatory macrophage response. Nature *488*, 404–408.

Kuzmichev, A., Nishioka, K., Erdjument-Bromage, H., Tempst, P., and Reinberg, D. (2002). Histone methyltransferase activity associated with a human multiprotein complex containing the Enhancer of Zeste protein. Genes Dev. *16*, 2893–2905.

Kuzmichev, A., Jenuwein, T., Tempst, P., and Reinberg, D. (2004). Different EZH2-containing complexes target methylation of histone H1 or nucleosomal histone H3. Mol. Cell *14*, 183–193.

Lagarou, A., Mohd-Sarip, A., Moshkin, Y.M., Chalkley, G.E., Bezstarosti, K., Demmers, J.A., and Verrijzer, C.P. (2008). dKDM2 couples histone H2A ubiquitylation to histone H3 demethylation during Polycomb group silencing. Genes Dev. *22*, 2799–2810.

Lau, P.N., and Cheung, P. (2011). Histone code pathway involving H3 S28 phosphorylation and K27 acetylation activates transcription and antagonizes polycomb silencing. Proc. Natl. Acad. Sci. USA *108*, 2801–2806.

Lee, J.M., Lee, J.S., Kim, H., Kim, K., Park, H., Kim, J.Y., Lee, S.H., Kim, I.S., Kim, J., Lee, M., et al. (2012). EZH2 generates a methyl degron that is recognized by the DCAF1/DDB1/CUL4 E3 ubiquitin ligase complex. Mol. Cell *48*, 572–586.

Luger, K., Rechsteiner, T.J., and Richmond, T.J. (1999). Expression and purification of recombinant histones and nucleosome reconstitution. Methods Mol. Biol. *119*, 1–16.

Margueron, R., and Reinberg, D. (2011). The Polycomb complex PRC2 and its mark in life. Nature *469*, 343–349.

Margueron, R., Justin, N., Ohno, K., Sharpe, M.L., Son, J., Drury, W.J., 3rd, Voigt, P., Martin, S.R., Taylor, W.R., De Marco, V., et al. (2009). Role of the polycomb protein EED in the propagation of repressive histone marks. Nature *461*, 762–767.

McKay, D.J., Klusza, S., Penke, T.J., Meers, M.P., Curry, K.P., McDaniel, S.L., Malek, P.Y., Cooper, S.W., Tatomer, D.C., Lieb, J.D., et al. (2015). Interrogating the function of metazoan histones using engineered gene clusters. Dev. Cell *32*, 373–386.

Min, J., Zhang, Y., and Xu, R.M. (2003). Structural basis for specific binding of Polycomb chromodomain to histone H3 methylated at Lys 27. Genes Dev. *17*, 1823–1828.

Müller, J., and Verrijzer, P. (2009). Biochemical mechanisms of gene regulation by polycomb group protein complexes. Curr. Opin. Genet. Dev. *19*, 150–158.

Müller, J., Hart, C.M., Francis, N.J., Vargas, M.L., Sengupta, A., Wild, B., Miller, E.L., O'Connor, M.B., Kingston, R.E., and Simon, J.A. (2002). Histone methyltransferase activity of a Drosophila Polycomb group repressor complex. Cell *111*, 197–208.

Munari, F., Soeroes, S., Zenn, H.M., Schomburg, A., Kost, N., Schröder, S., Klingberg, R., Rezaei-Ghaleh, N., Stützer, A., Gelato, K.A., et al. (2012). Methylation of lysine 9 in histone H3 directs alternative modes of highly dynamic interaction of heterochromatin protein hHP1β with the nucleosome. J. Biol. Chem. *287*, 33756–33765.

O'Meara, M.M., and Simon, J.A. (2012). Inner workings and regulatory inputs that control Polycomb repressive complex 2. Chromosoma *121*, 221–234.

Pasini, D., Bracken, A.P., Jensen, M.R., Lazzerini Denchi, E., and Helin, K. (2004). Suz12 is essential for mouse development and for EZH2 histone methyltransferase activity. EMBO J. *23*, 4061–4071.

Pattatucci, A.M., and Kaufman, T.C. (1991). The homeotic gene Sex combs reduced of Drosophila melanogaster is differentially regulated in the embryonic and imaginal stages of development. Genetics *129*, 443–461.

Pengelly, A.R., Copur, Ö., Jäckle, H., Herzig, A., and Müller, J. (2013). A histone mutant reproduces the phenotype caused by loss of histone-modifying factor Polycomb. Science *339*, 698–699.

Sanulli, S., Justin, N., Teissandier, A., Ancelin, K., Portoso, M., Caron, M., Michaud, A., Lombard, B., da Rocha, S.T., Offer, J., et al. (2015). Jarid2 Methylation via the PRC2 Complex Regulates H3K27me3 Deposition during Cell Differentiation. Mol. Cell *57*, 769–783.

Sawicka, A., Hartl, D., Goiser, M., Pusch, O., Stocsits, R.R., Tamir, I.M., Mechtler, K., and Seiser, C. (2014). H3S28 phosphorylation is a hallmark of the transcriptional response to cellular stress. Genome Res. *24*, 1808–1820.

Scheuermann, J.C., de Ayala Alonso, A.G., Oktaba, K., Ly-Hartig, N., McGinty, R.K., Fraterman, S., Wilm, M., Muir, T.W., and Müller, J. (2010). Histone H2A deubiquitinase activity of the Polycomb repressive complex PR-DUB. Nature *465*, 243–247.

Schmitges, F.W., Prusty, A.B., Faty, M., Stützer, A., Lingaraju, G.M., Aiwazian, J., Sack, R., Hess, D., Li, L., Zhou, S., et al. (2011). Histone methylation by PRC2 is inhibited by active chromatin marks. Mol. Cell *42*, 330–341.

Schuettengruber, B., Chourrout, D., Vervoort, M., Leblanc, B., and Cavalli, G. (2007). Genome regulation by polycomb and trithorax proteins. Cell *128*, 735–745.

Sengoku, T., and Yokoyama, S. (2011). Structural basis for histone H3 Lys 27 demethylation by UTX/KDM6A. Genes Dev. *25*, 2266–2277.

Shao, Z., Raible, F., Mollaaghababa, R., Guyon, J.R., Wu, C.T., Bender, W., and Kingston, R.E. (1999). Stabilization of chromatin structure by PRC1, a Polycomb complex. Cell *98*, 37–46.

Simon, J.A., and Kingston, R.E. (2013). Occupying chromatin: Polycomb mechanisms for getting to genomic targets, stopping transcriptional traffic, and staying put. Mol. Cell *49*, 808–824.

Steffen, P.A., Fonseca, J.P., Gänger, C., Dworschak, E., Kockmann, T., Beisel, C., and Ringrose, L. (2013). Quantitative in vivo analysis of chromatin binding of Polycomb and Trithorax group proteins reveals retention of ASH1 on mitotic chromatin. Nucleic Acids Res. *41*, 5235–5250.

Wei, H., and Zhou, M.M. (2010). Dimerization of a viral SET protein endows its function. Proc. Natl. Acad. Sci. USA *107*, 18433–18438.

Wolff, T. (2011). Preparation of Drosophila eye specimens for scanning electron microscopy. Cold Spring Harb. Protoc. *2011*, 1383–1385.

Yao, L.C., Liaw, G.J., Pai, C.Y., and Sun, Y.H. (1999). A common mechanism for antenna-to-Leg transformation in Drosophila: suppression of homothorax transcription by four HOM-C genes. Dev. Biol. *211*, 268–276.

Cell Reports

Supplemental Information

Histone H3 Serine 28 Is Essential for Efficient Polycomb-Mediated Gene Repression in *Drosophila*

Philip Yuk Kwong Yung, Alexandra Stuetzer, Wolfgang Fischle, Anne-Marie Martinez, and Giacomo Cavalli

Supplemental Information

Supplemental Figures S1-S4

- **Figure S1, Related to Figure 1. Schematic overview of the system for assaying the function of H3S28 and validation on histone replacement clones in larval imaginal discs.**
- **Figure S2, related to Figure 2. Hox gene derepression profiles in histone mutants (*H3S28A* and *H3K27R*) clones and *Antp*^{Ns}.**
- **Figure S3, related to Figure 3. Validation of clone induction of *dUtxΔ, H3S28A* double mutant and of in vivo RNAi against Aurora B kinase.**
- **Figure S4, related to Figure 2. Nuclear staining patterns of Ph remain unchanged in *H3S28A* mutant.**

Supplemental Figure Legends S1-S4

Supplemental Experimental Procedures

Supplemental References

Supplemental Figures
Figure S1

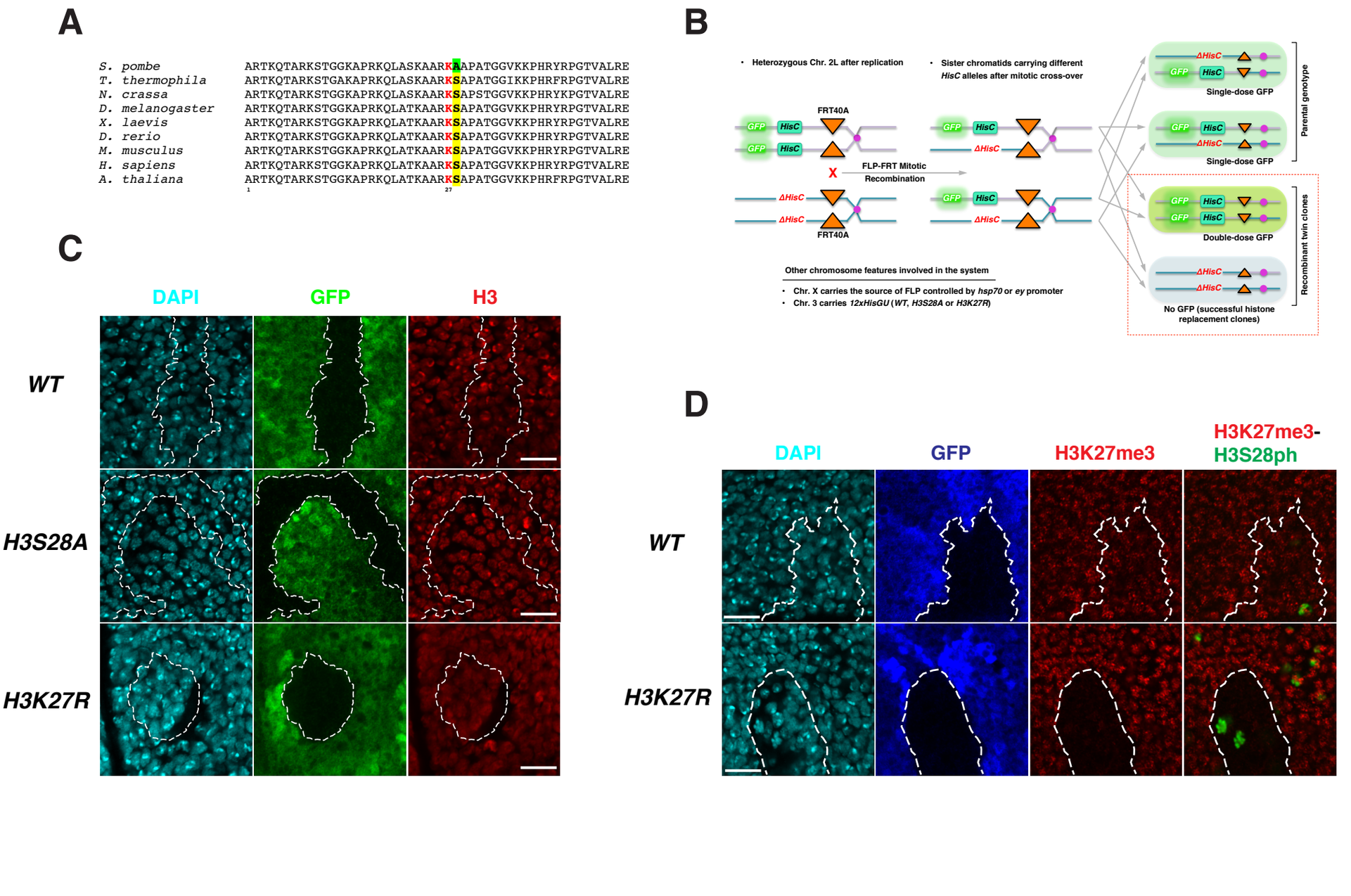

Figure S2

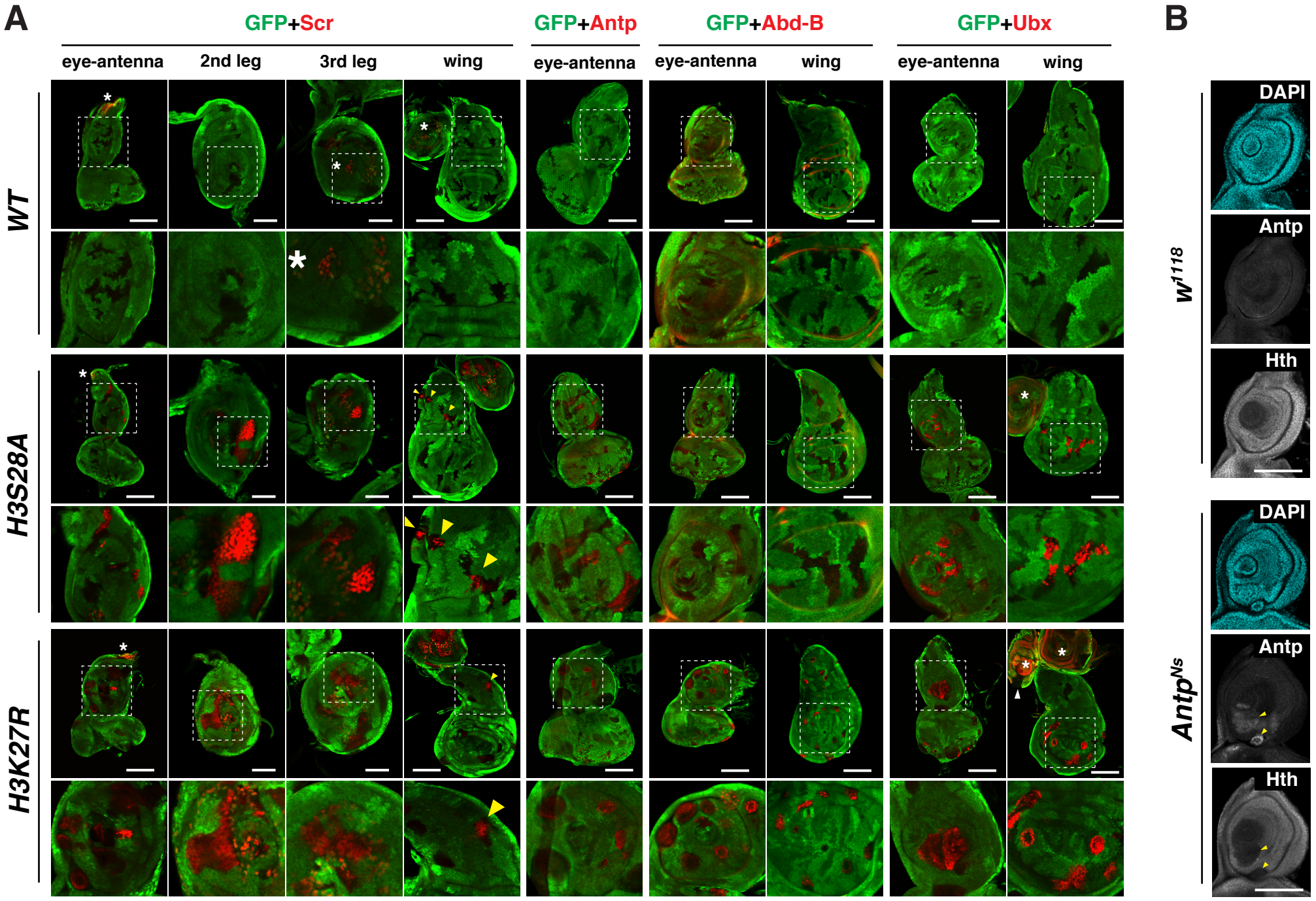
A
GFP+Scr
GFP+Antp
GFP+Abd-B
GFP+Ubx
eye-antenna
2nd leg
3rd leg
wing
eye-antenna
eye-antenna
wing
eye-antenna
wing
WT
H3S28A
H3K27R
B
w1118
Antp Ns
DAPI
Antp
Hth
DAPI
Antp
Hth

Figure S3

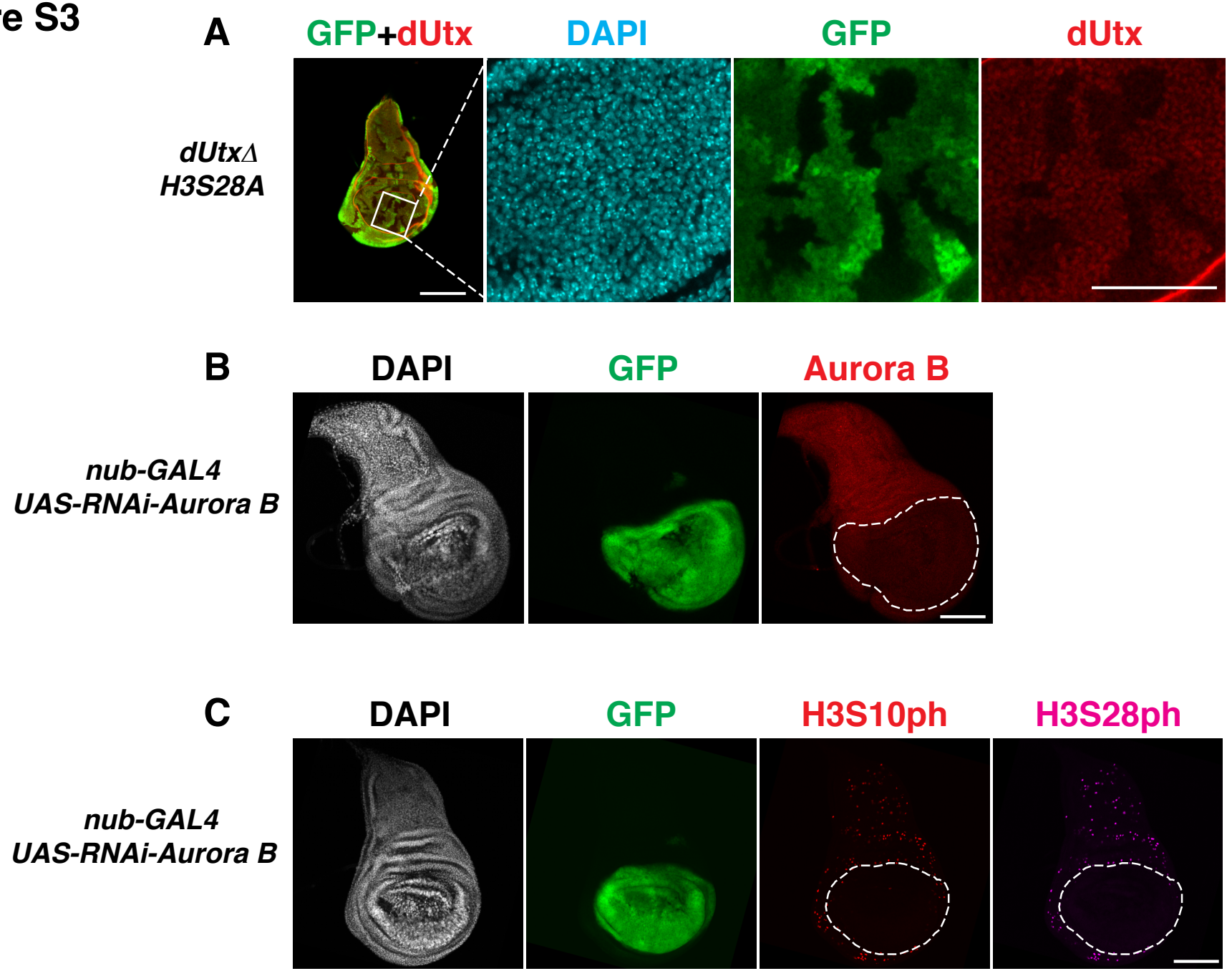
A
GFP+dUtx
DAPI
GFP
dUtx
dUtxΔ
H3S28A
B
DAPI
GFP
Aurora B
nub-GAL4
UAS-RNAi-Aurora B
C
DAPI
GFP
H3S10ph
H3S28ph
nub-GAL4
UAS-RNAi-Aurora B

Figure S4

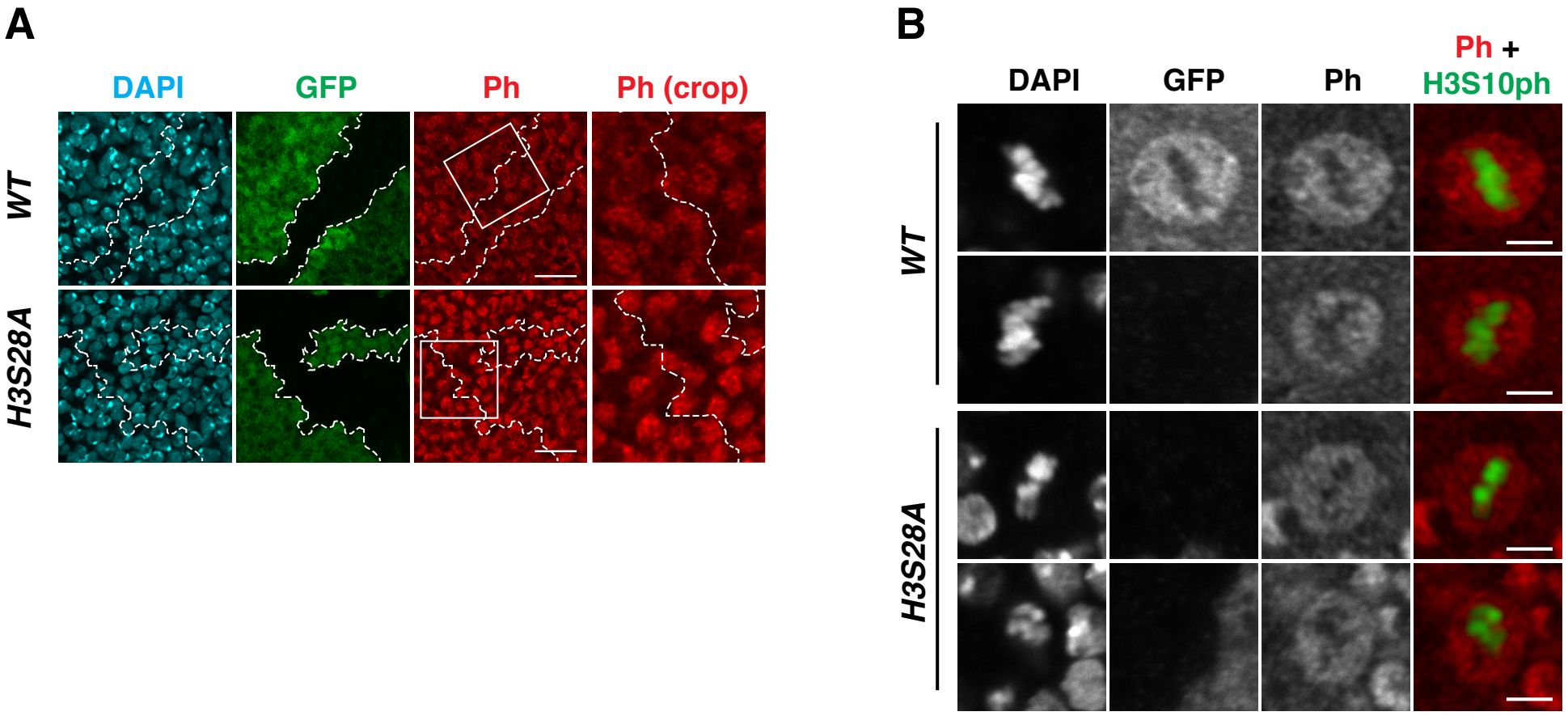
A
DAPI
GFP
Ph
Ph (crop)
WT
H3S28A
B
DAPI
GFP
Ph
Ph +
H3S10ph
WT
H3S28A

Supplemental Figure Legends

Figure S1, Related to Figure 1. Schematic overview of the system for assaying the function of H3S28 and validation on histone replacement clones in larval imaginal discs.

(A) The serine residue at position 28 of the histone H3 protein is conserved. Alignment of the N-terminal 1-50 amino acids of H3 from various eukaryotes. H3K27, the methylation target site of PRC2, is highlighted in red; the conserved H3S28 residue is highlighted in yellow and the variant alanine is highlighted in green. (B) Principle of mosaic analysis of *Drosophila* histone mutants. Inductions of mosaic histone mutant clones begin with parental cells that are heterozygous for the histone locus. Mitotic crossover occurs at FRT40A with the supply of FLP. And upon appropriate segregation of sister chromatids (bottom box in the right part of the figure), homozygous *HisC* alleles either in WT or deleted forms can be generated. Because of their co-emergence, they are also referred to as twin clones. Homozygous *ΔHisC* clones are marked by the lack of GFP, while twin WT HisC clones show twice the GFP expression compared to the surrounding heterozygous cells. Since chromosome 3 is integrated with 12xHisGU, the endogenous source of H3 can be replaced by different H3 alleles in the *ΔHisC* clones. (*C*) and (*D*) Wing imaginal discs of homozygous *ΔHisC* clones supplemented with 12xHisGU transgenes carrying either H3 *WT*, *H3S28A* or *H3K27R* alleles. Immunostaining with the indicated antibodies is shown; DNA was stained with DAPI. Clones of interest are marked by the lack of GFP signal and are indicated by dashed lines. (*C*) Comparison of H3 staining in WT (GFP positive) tissue with clones containing *WT*, *H3S28A* or *H3K27R* histone replacement. Note that all histone replacement clones displayed normal H3 staining (red) level similar to the surrounding GFP positive (green) cells. (*D*) Comparison of H3K27me3 (red) levels in GFP-negative (histone replacement) clones with GFP-positive normal tissue. Note that *H3K27R* mutant cells (bottom row) were depleted of H3K27me3 despite having normal mitotic H3S28ph signal (green). *WT* clones supported robust H3K27me3 levels indistinguishable from the surrounding GFP positive cells. For clarity of composite micrographs, GFP is pseudocolored to blue in (*D*). Scale bars correspond to 10 μm.

Figure S2, related to Figure 2. Hox gene derepression profiles in histone mutants (*H3S28A* and *H3K27R*) clones and *Antp*^{Ns}.

(A) Micrographs showing full-scale imaginal discs described in Figure 2 and main text. For each imaginal disc, a selected region (dashed line) is magnified and displayed below the corresponding micrograph. Asterisks mark zones of endogenous expression of Scr and Ubx. Yellow arrowheads highlight weak Scr derepression occasionally detected in the notum region of wing discs in both *H3S28A* and *H3K27R* mutant clones. The white arrowhead indicates ectopic silencing of endogenous Ubx expression in the haltere disc carrying *H3K27R* clones. Scale bars of wing and eye-antenna discs represent 100 μm and those of leg discs represent 50 μm. (B) Antennal discs of w^{1118} (top panel) and *Antp*^{Ns} (bottom panel) were immunostained with the indicated antibodies. DNA was stained with DAPI. Arrowheads indicate ectopic expression of Antp and silencing of the antennal selector gene Hth. Scale bar corresponds to 100 μm.

Figure S3, related to Figure 3. Validation of clone induction of *dUtxΔ, H3S28A* double mutant and of in vivo RNAi against Aurora B kinase.

(A) Wing imaginal discs with clones homozygous of the combined *dUtxΔ, H3S28A* mutants were immunostained with the indicated antibodies. DNA was stained by DAPI. Clones were marked by the absence of GFP, which correspond to a drastic reduction of dUtx signal. (B) and (C) *Drosophila* wing imaginal discs of L3 larva with *nub-GAL4* directed RNAi against Aurora B at the wing pouch compartment marked by GFP and dotted lines. Wing discs were immunostained with the indicated antibodies and DNA was stained with DAPI. Scale bar of full-disc micrograph represents 100 μm and those of magnified regions in (*A*) represents 40 μm.

Figure S4, related to Figure 2. Nuclear staining patterns of Ph remain unchanged in *H3S28A* mutant.

(A) Immunostaining of wing imaginal discs for Ph. *WT* (top row) and *H3S28A* (bottom row) clones are identified by the lack of GFP signal and are marked by dashed lines. Samples were stained with DAPI and the indicated antibodies. Regions at the clone borders were further cropped and magnified. (B) Selections of mitotic cells from *WT* and *H3S28A* clones in wing imaginal discs were compiled to show the distribution of Ph during mitosis in the corresponding backgrounds. Only GFP-positive internal controls of *WT* clones are shown. Scale bars in (A) and (B) represent 10 μm and 2.5 μm, respectively.

Supplemental Experimental Procedures

***Drosophila* Stocks**

The following fly lines were used in this study

y, w; P{Ubi-GFP.D}33, P{Ubi-GFP.D}38, FRT40A (Bloomington #BL5189)

y, w, hsp70-flp; Df(2L) BSC104, FRT40A/CyO, twist-Gal4, UAS-GFP; MKRS/TM6B (Hodland Basler, 2012)

y, w; dUtxΔ, FRT40A/CyO, twist-Gal4, UAS-GFP (Copur and Muller, 2013)

y, w, hsp70-flp122; P{Ubi-GFP.D}33, P{Ubi-GFP.D}38, FRT40A; 6xHisGU

y, w, hsp70-flp122; P{Ubi-GFP.D}33, P{Ubi-GFP.D}38, FRT40A; 6xHisGU^{H3S28A}

y, w, hsp70-flp122; P{Ubi-GFP.D}33, P{Ubi-GFP.D}38, FRT40A; 6xHisGU^{H3K27R}

w; Df(2L) BSC104, FRT40A /CyO, Kr-Gal4, UAS-GFP; 6xHisGU

w; Df(2L) BSC104, FRT40A /CyO, Kr-Gal4, UAS-GFP; 6xHisGU^{H3S28A}

w; Df(2L) BSC104, FRT40A /CyO, Kr-Gal4, UAS-GFP; 6xHisGU^{H3K27R}

w; dUtxΔ, Df(2L) BSC104, FRT40A /CyO, Kr-Gal4, UAS-GFP; 6xHisGU

w; dUtxΔ, Df(2L) BSC104, FRT40A /CyO, Kr-Gal4, UAS-GFP; 6xHisGU^{H3S28A}

y, w, ey-FLP1; P{Ubi-GFP.D}33, P{Ubi-GFP.D}38, FRT40A; 6xHisGU

y, w, ey-FLP1; P{Ubi-GFP.D}33, P{Ubi-GFP.D}38, FRT40A; 6xHisGU^{H3S28A}

y, w ey-FLP1; P{Ubi-GFP.D}33, P{Ubi-GFP.D}38, FRT40A; 6xHisGU^{H3K27R}

Antp^{Ns}/TM3, Ser (Kindly provided by Walter Gehring lab.)

w^{1118}

Mosaic analysis and Immunostaining

Primary antibodies used for immunostaining in this study:Hox antibodies were purchased from the Developmental Studies Hybridoma Bank (DSHB). Mouse anti-Scr (DSHB 6H4.1, 1:20), mouse anti-Antp (DSHB 8C11, 1:20), mouse anti-Ubx (DSHB FP3.38, 1:20), mouse anti-Abd-B (DSHB 1A2E9, 1:10), mouse anti-En (DSHB 4D9, 1:20), mouse anti-H3 (ActiveMotif 39763, 1:500), mouse antiH3S10ph (Millipore 05-806, 1:1000), rat anti-H3S28ph (Millipore MABE76, 1:1000), rabbit anti-H3K27me3 (Millipore 07-449, 1:500), rabbit anti-H3K27me2 (Upstate 07-452, 1:500), rabbit anti-H3K27me1 (Millipore 07-448, 1: 250), rabbit anti-H3K27ac (Abcam Ab4729, 1:500), rabbit anti-H34me3 (Millipore 04-745, 1:500), rabbit anti-Pc ((Grimaud et al., 2006), 1:500), goat anti-Ph ((Grimaud et al., 2006), 1:500), guinea pig anti-Hth (a gift from Ginés Morata, 1:200), rabbit anti- Aurora B (a gift from David Glover, 1: 200), rabbit anti-dUtx (a gift from Feng Tie and Peter J. Harte, 1: 200) chicken anti-GFP (Invitrogen A10262, 1:500).

Supplemental References

Copur, O., and Muller, J. (2013). The histone H3-K27 demethylase Utx regulates HOX gene expression in Drosophila in a temporally restricted manner. Development *140*, 3478-3485.
Grimaud, C., Bantignies, F., Pal-Bhadra, M., Ghana, P., Bhadra, U., and Cavalli, G. (2006). RNAi components are required for nuclear clustering of Polycomb group response elements. Cell *124*, 957-971.
Hodl, M., and Basler, K. (2012). Transcription in the absence of histone H3.2 and H3K4 methylation. Curr Biol *22*, 2253-2257.